Applications and Challenges of Reverse Time Migration of Multiples

Zhiping Yang*, Jeshurun Hembd (CGG)

Abstract

In many processing flows for marine streamer data, free-surface multiples are regarded as noise and significant efforts are made to remove them. However, this multiple wavefield actually contains additional information that can be useful, particularly for illuminating shallow and/or complex structures.

We recently modified our reverse time migration (RTM) algorithm, enabling it to image correctly between the primary wavefield and the first-order multiple wavefield. We call this modification reverse time migration of multiples (RTMM). We demonstrate that RTMM can take advantage of the extra illumination of the multiple wavefield to produce better or complementary images in shallow-water areas and in regions with complex salt structures. We also explore one of the major challenges of RTMM, which is crosstalk noise, and discuss some tactics for addressing it.

Introduction

Even with an increasing amount of surface offset and azimuthal coverage from modern marine streamer acquisition configurations, we may still lack sufficient illumination by the primary wavefield in certain geologic scenarios. Two common problems include shallow water where the water bottom primary reflection can be poorly recorded and regions of complex salt where the geology can create erratic reflection patterns that may lead to illumination dim zones in primary migration images. Yang et al. (2013) demonstrated that the source illumination of a single shot by RTMM is much more widespread and balanced than its primary-only wavefield complement RTM. Instead of treating the multiple wavefield as noise, we seek to harness its additional illumination information.

Some attempts have been made to utilize the multiple wavefield in imaging (Berkhout and Verschuur, 1994; Liu et al., 2010; Lu et al., 2011). These methods are similar in principle but differ in details. They may differ in the exact choice for the source and/or receiver wavefields as well as the wave propagation engines, such as one-way or two-way wave-equation migration algorithms. We chose to forward propagate the recorded primary data as the source wavefield and backward propagate the recorded first-order multiple data as the receiver wavefield. Our propagation engine is the two-way migration algorithm of RTM.

We first demonstrate how this method effectively improves imaging of a shallow water bottom by assisting in model-based water-layer demultiple (MWD) (Wang et al., 2011). Then, we demonstrate how the RTMM complement to an RTM image can assist with structural image interpretation.

One of the major challenges of RTMM is crosstalk noise. We examine this phenomenon and classify crosstalk noise into two different categories. Using synthetic data, we dissect each category and then discuss possible methods to handle them.

Method

To prepare the input for RTMM, we must isolate the primaries and the first-order multiples from the recorded data. First, we apply the standard surface-related multiple elimination (SRME) (Verschuur, 1992) to predict all orders of multiples. Subtraction of these multiples from the recorded data yields the primaries. These primaries are then convolved with the subtracted multiples to predict the second and higher orders of multiples. The subtraction of these high-order multiples from the total multiple model yields the desired first-order multiples.

Once the input is ready, the modification to the RTM algorithm is fairly straightforward. Standard RTM forward propagates an impulse from the shot location to simulate the source wavefield and backward propagates the recorded primary for the receiver wavefield. After both wavefields are propagated, an imaging condition is applied to form a seismic image. For RTMM, we forward propagate the recorded primary data for the source wavefield and backward propagate the recorded first-order multiple data for the receiver wavefield. Once both wavefields are propagated, a similar imaging condition is applied to obtain the image.

RTMM for Shallow Imaging and MWD

In shallow water surveys, data coverage at near offsets may be limited. This lack of near angle reflections brings two challenges for imaging. First, the poor sampling of key shallow primaries can limit the performance of multiple attenuation because common convolution-based methods, such as SRME, require well-recorded near offset data (Verschuur, 1992). Second, the missing data is very apparent in the migrated image, especially at the water bottom (Figure 1a). In this situation, RTMM can help image shallow reflectors by using near angle reflections from the multiple wavefield. The improved shallow image can be used to derive accurate water bottom reflection information, which can then improve multiple attenuation using MWD (Wang, 2011).
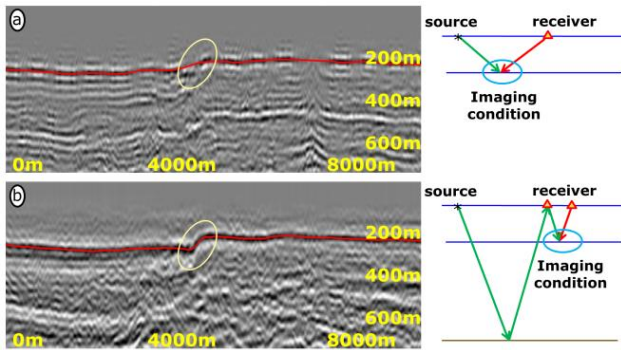
Figure 1: Water flood images (crossline view) of (a) reverse time migration (RTM) and (b) reverse time migration of multiples (RTMM) along with their corresponding schematic ray path diagrams.

We illustrate this strategy with a real data example from a wide azimuth (WAZ) survey in the Gulf of Mexico. Figure 1 compares standard RTM and RTMM water flood images in the crossline view from a shallow water region near the border of East Breaks and Garden Banks. Applying standard RTM resulted in an obvious acquisition footprint in the crossline view with poorly imaged stripes appearing approximately every 600 m between each sail line, whereas RTMM resulted in a focused and continuous water bottom. The schematic ray path diagrams next to the corresponding images explain this dramatic difference. For RTM, the reflection angle from the water bottom reached critical angle quickly as the receivers extended in the crossline direction. This stretched the water bottom wavelet and reduced its amplitude, introducing alternating patterns of strong and weak amplitudes. For RTMM, the energy illuminating the water bottom was no longer limited to impulses from the sparse shot locations. Instead, all the recorded primary energy was used to illuminate the water bottom from the relatively dense receiver locations. Primary energy from the deep subsurface structures can be especially useful for generating a significantly smaller reflection angle at the water bottom. These additional small angle reflections available to RTMM helped define details about the water bottom horizon (yellow circle) that would have been completely missed using standard RTM. The red lines in Figure 1 mark the water bottom horizons obtained by auto-tracking using the same parameters.

We generated the water bottom horizons from the two
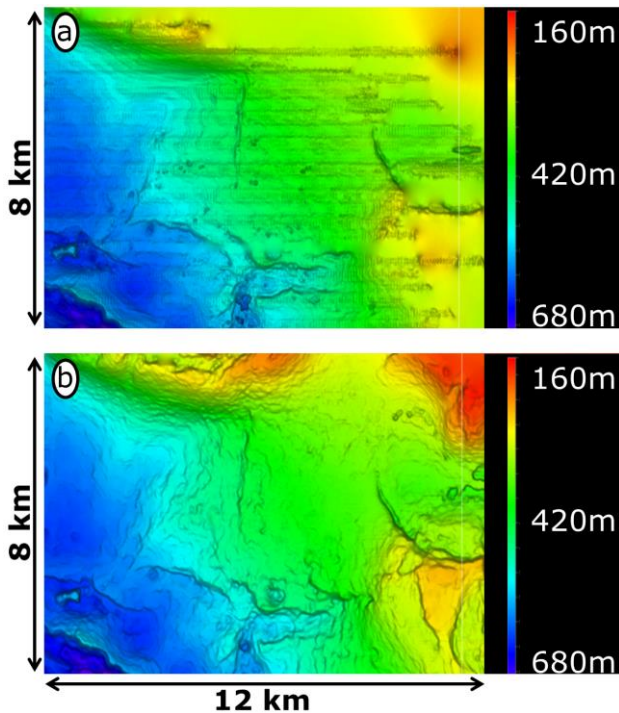

Figure 2: Water bottom horizon generated from the (a) standard RTM image and (b) RTMM image. Color represents water bottom depth.
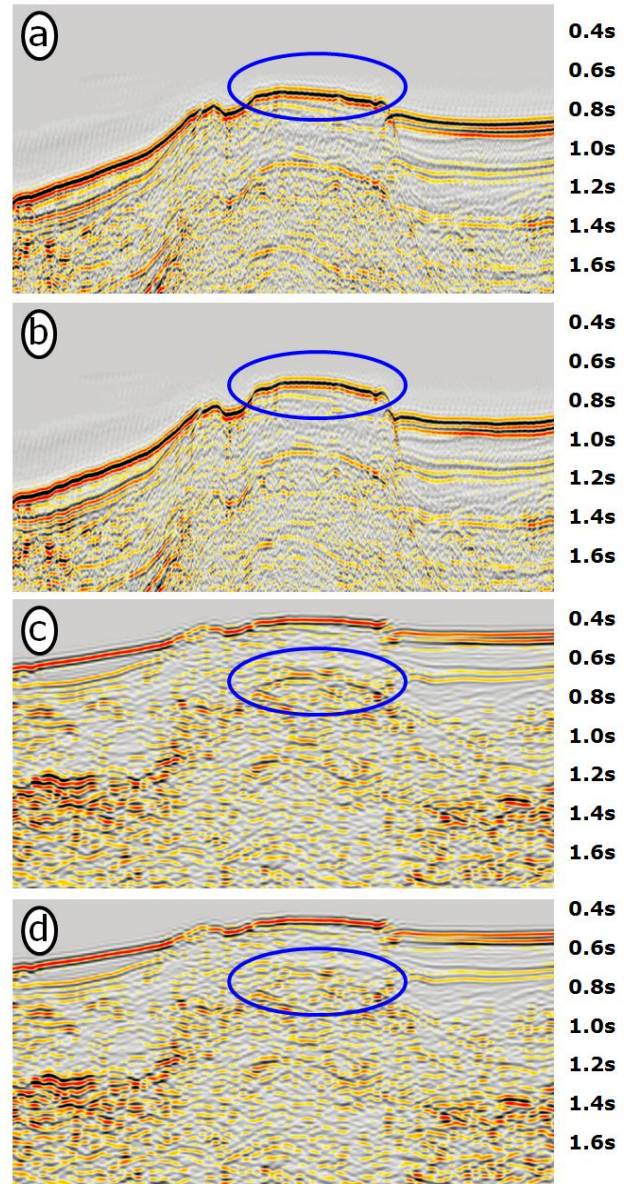

Figure 3: Near channel MWD results. Multiples predicted using a horizon interpreted from (a) standard RTM and (b) RTMM. Demultiple output using water bottom horizon determined by (c) standard RTM and (d) RTMM.

water flood images in Figure 1 (Figure 2). The standard RTM water bottom horizon (Figure 2a) showed a number of horizontal stripes (i.e., the acquisition footprint). In comparison, the RTMM water bottom horizon (Figure 2b) was nearly artifact-free with high-resolution details of the water bottom topography.

We can create a more precise multiple model from the RTMM-generated horizon and thus a cleaner data set after MWD. Figure 3 shows the MWD multiple models based on the two horizons: the horizon interpreted on the standard RTM image (Figure 3a) and the horizon interpreted on the RTMM image (Figure 3b). The corresponding demultiple outputs are shown in Figures 3c and 3d, respectively. The residual multiple is less obvious in Figure 3d than in Figure 3c.

RTMM for complementary illumination

Using the same data set, we tested RTMM for its illumination assistance. Even in surveys with surface data extending far enough to provide ample apertures for imaging (e.g., many WAZ surveys), some complex salt geometries may still suffer from less-than-optimal illumination. In these cases, the multiple wavefield may provide complementary illumination, which can assist in salt body delineation and structural interpretation.

Figure 4 shows a real data, full-volume stacked image (crossline view) comparison between standard RTM (Figure 4a) and RTMM (Figure 4b). The yellow curves above the water bottom in Figures 4a and 4b are the extracted water bottom amplitudes from each migration. The acquisition footprint is visible again in the water bottom amplitude extraction by standard RTM. In comparison, the RTMM result suffers much less from this problem. Figures 4c and 4d gives a bird's-eye view of the extracted water bottom amplitudes from RTM and RTMM, respectively. The black lines in Figures 4c and 4d indicate the location of the crossline for Figures 4a and 4b, respectively.

In the complementary RTMM image (Figure 4), the blue arrows indicate locations where RTMM provided a better top of salt, shallow sediment, overhang base, and certain parts of the base of salt compared to standard RTM. These complementary images can augment our understanding of the geologic structure and help with interpretation.

Understanding the crosstalk noise

To understand crosstalk noise, we conducted a 2D study on two synthetic models: the Sigsbee2b and a flat reflector model. We classified the crosstalk noise into two categories: (1) cross-order crosstalk and (2) cross-event crosstalk.
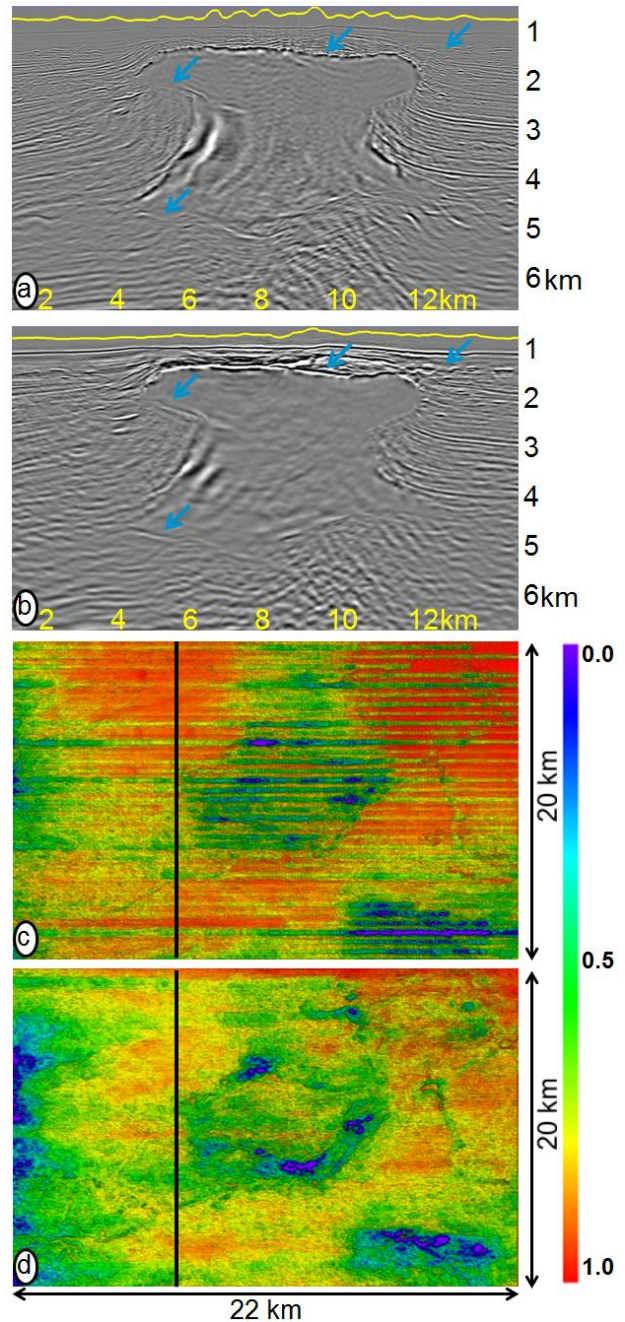

Figure 4: Real data full-volume stacked images (crossline view) of (a) RTM and (b) RTMM. Extracted water bottom amplitude from (c) RTM and (d) RTMM. Color represents normalized water bottom amplitude.
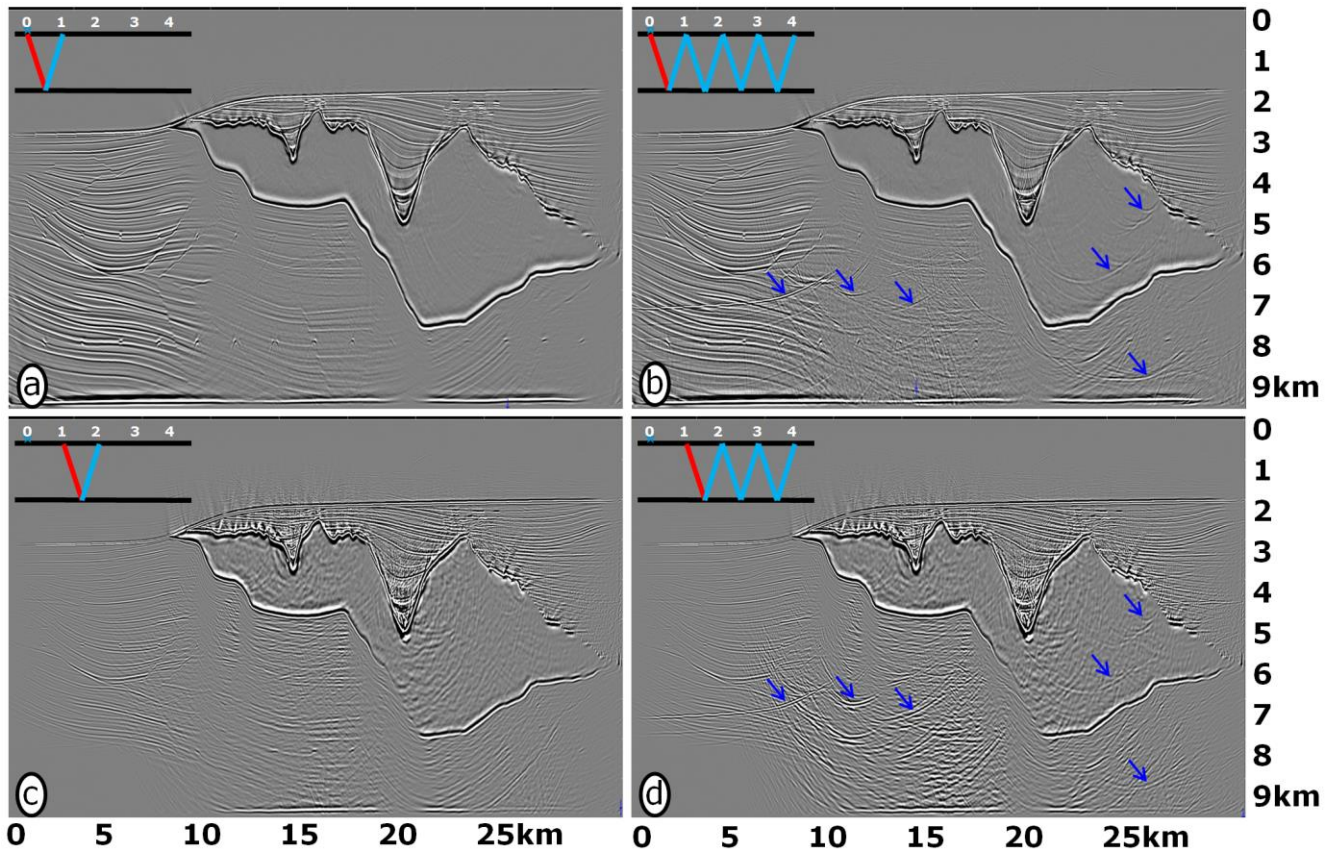
Figure 5: Study of cross-order crosstalk noise on Sigsbee2b model. (a) Standard RTM "0 * 1" without multiple. (b) Standard RTM "0 * 1+2+3+4" with multiple. (c) RTMM "1 * 2" without higher-order multiple. (d) RTMM "1 * 2+3+4" with higher-order multiple.

Cross-order crosstalk occurs between different orders of multiples. For this type of crosstalk noise, the impulse wavefield from shot location is "order = 0", the primary wavefield is "order = 1", the first-order multiple is "order = 2", etc. Standard RTM applied an imaging condition between order "0" and "1", (abbreviated as "0 * 1") (Figure 5a), whereas RTMM applied an imaging condition abbreviated as "1* 2" (Figure 5c). The majority of the crosstalk noise in RTMM is cross-order crosstalk "1* 3+4" (Figure 5d). In this unified picture, the multiple artifacts in standard RTM are also viewed as cross-order crosstalk noise "0 * 2+3+4" (Figure 5b). In fact, the ray paths in Figures 5b and 5d are nearly identical, and the positions of the noise in the stacked images match well with each other (blue arrows). Thus, the natural strategy for handling cross-order crosstalk noise is to separate different orders of multiples and apply imaging conditions only to the pairs that may form a correct image (receiver side has one order higher than the source side).

The second type of crosstalk noise, cross-event crosstalk, is formed by the complexity of the down-going wavefield and can be more difficult to handle. To illuminate the challenges associated with this type of crosstalk, we studied a simple synthetic model of multiple events imaging one flat reflector. Figure 6a shows the density model with two closely spaced shallow flat reflectors and one deep flat reflector. The velocity model was one

constant value throughout. We attempted to use the reflected primary wavefield from the shallow reflectors to image the deep reflector with RTMM.

To simplify the demonstration, we selected the data that matches the green ray paths for the primary (source) wavefield (order "1") and blue ray paths for the first-order multiple (receiver) wavefield (order "2"). An interbed event between the two shallow reflectors was unavoidably included (far right of the ray path diagram). There was no cross-order crosstalk here, and the image was formed solely by primaries and first-order multiples ("1 * 2"). However, cross-event crosstalk was generated once several events illuminated the same reflector. There were several artificial layers in the RTMM image (Figure 6b). To understand how cross-event crosstalk noise was generated, we overlaid snapshots of the source and receiver wavefields. If a down-going source wavefront only "sees" its own reflected up-going wavefront in the receiver wavefield, it forms an image free of crosstalk. However, the same source wavefront typically intersects with many other receiver wavefronts generated by neighboring events and vice versa. Those "mismatched" pairs of source and receiver wavefronts are the root cause of cross-event crosstalk.

The practical approach we used to deal with cross-event crosstalk noise in real data is to produce the vector offset output (VOO) (Xu et al., 2011). VOO sectors effectively
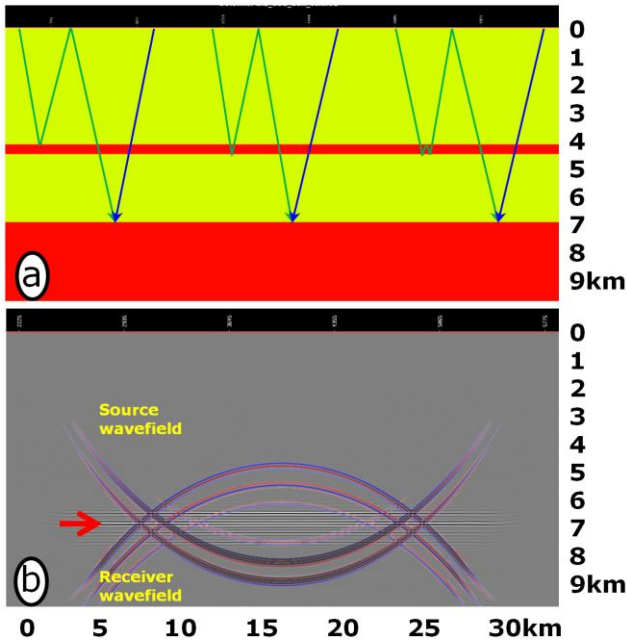
Figure 6: Study of cross-event crosstalk noise on a flat reflector model. (a) Density model overlaid with selected ray paths for source (green) and receiver (blue) wavefields. (b) RTMM image overlaid with source and receiver wavefields at a given time step. The red arrow points to the true location of the flat reflector to be imaged.

decompose a stack image into separate dip components. With the help of a guiding reference volume or reference dip field, the VOO sectors use a coherence metric or structure conformal filtering to merge back to a final stack image. However, cross-event crosstalk is still a significant challenge in areas where the geology is mostly flat and/or has parallel dips.

Conclusions

We modified the standard RTM algorithm to enable correct imaging between the recorded primary wavefield and the first-order multiple wavefield. We named our approach RTMM. Due to the abundant small angle reflections of RTMM, we were able to obtain an accurate water bottom even in a shallow water area where it can be difficult for standard RTM due to missing near-offset data. Obtaining an accurate water bottom enables us to improve upon MWD demultiple results. Additionally, in areas of complex geology, we can use the more widespread illumination power of RTMM over RTM to generate complementary images. These complementary images can assist with guiding salt body delineation and other structural interpretation efforts.

Every coin has two sides. While RTMM enjoys the illumination benefit of the multiple wavefield, it suffers from the crosstalk noise problem. We identified two separate classes of crosstalk and determined that they may each best be dealt with independently. The generally known cross-order crosstalk can be avoided by modeling and separating the various orders of multiples. The second type of crosstalk noise we discovered is the cross-event crosstalk. In areas of complex geology, we might assume that many of these interfering arrivals

originate from different directions. Thus, using *a priori* geologic knowledge, we were able to use VOO to separate the crosstalk noise from the true seismic image.

Although these crosstalk solutions have been reasonably successful in practice, no widely accepted solution exists to handle crosstalk noise in migration of multiples. Least-squares inversion is a good candidate, and there have been efforts in this direction with promising results using OBN data (Wong, 2014).

References

Berkhout A. J., and D. J. Verschuur, 1994, Multiple technology: Part 2, migration of multiple reflections: SEG Exp. Abstracts, SEG,1497–1500.

Berkhout A. J., and D. J. Verschuur, 2011, Full wavefield migration, utilizing surface and internal multiple scattering: SEG Exp. Abstracts, SEG, 3212-3216.

Liu, Y., X. Chang, D. Jin, R. He, H. Sun, and Y. Zheng, 2010, Reverse time migration of multiples for subsalt imaging: Geophysics, 76(5), WB209-WB216.

Lu, S., N. D. Whitmore, A. A. Valenciano, and N. Chemingui, 2011, Imaging of primaries and multiples with 3D SEAM synthetic: SEG Exp. Abstracts, SEG, 3217-3221.

Verschuur, D. J. and A.J. Berkhout, 1992, Surface-related multiple elimination: Practical aspects: SEG Exp. Abstracts, SEG, 1100-1103.

Wang, P., H. Jin, S. Xu, and Y. Zhang, 2011, Model-based water-layer demultiple: SEG Exp. Abstracts, SEG, 3551-3555.

Wong, M., B. Biondi, and S. Ronen, 2014, Imaging with multiples using least-squares reverse time migration: The Leading Edge, 33(9), 970-976.

Xu, Q., Y. Li, X. Yu, and Y. Huang, 2011, Reverse time migration using vector offset output to improve sub-salt imaging – a case study at the Walker Ridge GOM: SEG Exp. Abstracts, SEG, 3269-3274.

Yang, Z., L. Chernis, W. Gou, S. Ji, Y. Li, and J. Hembd, 2013, Enhanced reverse time multiple migration and its applications: SEG Exp. Abstracts, SEG, 4121-4125.